

# Some Stars are Totally Metal: A New Mechanism Driving Dust Across Star-Forming Clouds, and Consequences for Planets, Stars, and Galaxies

Philip F. Hopkins<sup>1</sup>\*

<sup>1</sup>TAPIR, Mailcode 350-17, California Institute of Technology, Pasadena, CA 91125, USA

Submitted to MNRAS, January, 2014

## ABSTRACT

Dust grains in neutral gas behave as aerodynamic particles, so they can develop large local density fluctuations entirely independent of gas density fluctuations. Specifically, gas turbulence can drive order-of-magnitude “resonant” fluctuations in the dust density on scales where the gas stopping/drag timescale is comparable to the turbulent eddy turnover time. Here we show that for large grains (size  $\gtrsim 0.1\ \mu\text{m}$ , containing most grain mass) in sufficiently large molecular clouds (radii  $\gtrsim 1\text{--}10\text{ pc}$ , masses  $\gtrsim 10^4 M_\odot$ ), this scale becomes longer than the characteristic sizes of pre-stellar cores (the sonic length), so large fluctuations in the dust-to-gas ratio are imprinted on cores. As a result, star clusters and protostellar disks formed in large clouds should exhibit substantial abundance spreads in the elements preferentially found in large grains (C, O). This naturally predicts populations of carbon-enhanced stars, certain highly unusual stellar populations observed in nearby open clusters, and may explain the “UV upturn” in early-type galaxies. It will also dramatically change planet formation in the resulting protostellar disks, by preferentially “seeding” disks with an enhancement in large carbonaceous or silicate grains. The relevant threshold for this behavior scales simply with cloud densities and temperatures, making straightforward predictions for clusters in starbursts and high-redshift galaxies. Because of the selective sorting by size, this process is not visible in extinction mapping. We also predict the shape of the abundance distribution – when these fluctuations occur, a small fraction of the cores are actually seeded with abundances  $Z \sim 100\langle Z \rangle$  such that they are almost “totally metal” ( $Z \sim 1$ )! Assuming the cores collapse, these totally metal stars would be rare (1 in  $\sim 10^4$  in clusters where this occurs), but represent a fundamentally new stellar evolution channel.

**Key words:** star formation: general — protoplanetary discs — galaxies: formation — galaxies: evolution — hydrodynamics — instabilities — turbulence — cosmology: theory

## 1 INTRODUCTION

For  $\sim 50$  years, essentially all models of star formation and molecular clouds have ignored a ubiquitous physical process – namely that massive dust grains naturally experience large density fluctuations in turbulent, neutral media (so-called “turbulent concentration”).

It has long been known that, in atomic/molecular gas, dust grains – which contain a large fraction of the heavy elements in the interstellar medium (ISM) – behave as aerodynamic particles. As such, below some characteristic size scale, they are effectively decoupled from the gas, and can (in principle) clump or experience density fluctuations independent from gas density fluctuations. But this process has largely been ignored in most of astrophysics. Recently, though, much attention has been paid to the specific question of grain density fluctuations and resulting “grain concentrations” in proto-planetary disks. When stirred by turbulence, the number density of solid grains can fluctuate by multiple orders of magnitude, even when the gas is strictly incompressible! This has been seen in a wide variety of simulations, with super and sub-sonic turbulence,

including or excluding the effects of grain collisions, and in non-magnetized and magnetically dominated media (see e.g. Bracco et al. 1999; Cuzzi et al. 2001; Johansen & Youdin 2007; Carballido et al. 2008; Bai & Stone 2010b,a,c; Pan et al. 2011). And grain clumping occurs similarly regardless of whether turbulent motions are self-excited (the “streaming” instability; Youdin & Goodman 2005), or externally driven via global gravitational instabilities, the magneto-rotational instability, convection, or Kelvin-Helmholtz instabilities (Dittrich et al. 2013; Jalali 2013).

In the terrestrial turbulence literature, this identical process (“preferential concentration” of aerodynamic particles) is very well studied. Actual laboratory experiments (Squires & Eaton 1991; Fessler et al. 1994; Rouson & Eaton 2001; Gualtieri et al. 2009; Monchaux et al. 2010), as well as numerical simulations (Cuzzi et al. 2001; Yoshimoto & Goto 2007; Hogan & Cuzzi 2007; Bec et al. 2009; Pan et al. 2011; Monchaux et al. 2012) have clearly demonstrated that turbulent gas is unstable to the growth of very large-amplitude inhomogeneities in the dust-to-gas ratio.

Here, we argue that the same physics should apply in star-forming molecular clouds, and argue that grain density fluctuations will occur at interesting levels in large clouds, with potentially rad-

\* E-mail: phopkins@caltech.edu

ical implications for star formation and stellar evolution, as well as planet formation in the disks surrounding those stars.

## 2 THE PHYSICS

### 2.1 Dust as Aerodynamic Particles

In a neutral medium, dust grains couple to gas via collisions with individual atoms/molecules (the long-range electromagnetic or gravitational forces from individual molecules are negligible). In the limit where the grain mass is much larger than the mass of an individual atom (grain size  $\gg \text{\AA}$ ), the stochastic nature of individual collisions is averaged out on an extremely short timescale, so the grain behaves as an aerodynamic particle. The equation of motion for an individual dust grain is the Stokes equation:

$$\frac{D\mathbf{v}}{Dt} = -\frac{\mathbf{v} - \mathbf{u}(\mathbf{r})}{t_s} + \frac{1}{m_{\text{grain}}} \mathbf{F}_{\text{ext}}(\mathbf{r}) \quad (1)$$

$$t_s \equiv \frac{\bar{\rho}_{\text{solid}} a}{\rho_g c_s} \quad (2)$$

where  $D/Dt$  denotes the Lagrangian (comoving) derivative,  $\mathbf{v}$  is the grain velocity,  $\mathbf{u}(\mathbf{r})$  is the local gas velocity,  $\bar{\rho}_{\text{solid}} \approx 2 \text{ g cm}^{-3}$  is the *internal* grain density (Weingartner & Draine 2001),  $a = a_\mu \mu\text{m} \sim 10^{-4} - 10$  is the grain size,  $\rho_g$  is the mean gas density,  $c_s$  the gas sound speed,<sup>1</sup> and  $\mathbf{F}_{\text{ext}}$  represents the long-range forces acting on the grains (e.g. gravity). It is important to note that most of the *mass* in dust, hence a large fraction of the total metal mass, is in the largest grains with  $a_\mu \sim 0.1 - 10$  (see Draine 2003, and references therein).<sup>2</sup>

Here  $t_s$  is the “stopping time” or “friction time” of the grain – it comes from the mean effect of many individual collisions with molecules in the limit  $m_{\text{grain}} \gg m_p$  (for a  $a_\mu \sim 1$ ,  $m_{\text{grain}} \sim 10^{13} m_p$ ).<sup>3</sup> On timescales  $\ll t_s$ , i.e. spatial scales  $\ll t_s |\mathbf{v}|$ , grains behave like collisionless particles (they do not “feel” pressure forces). It is only over timescales  $\gg t_s$  (spatial scales  $\gg t_s |\mathbf{v}|$ ) that the grains can be treated as tightly-coupled to the gas (e.g. as a fluid).

### 2.2 How Dust-to-Gas Fluctuations Occur

Because of this, grains can in principle fluctuate in density *relative to the gas*. We illustrate this with a simple test problem in Fig. 1. Consider a turbulent eddy – for simplicity, imagine a vortex in pure circulation  $\mathbf{u} = u_e \hat{\phi} = (r_e/t_e) \hat{\phi}$ , where  $u_e$ ,  $r_e$ ,  $t_e = r_e/|u_e|$  are the characteristic eddy velocity, size, and “turnover time” (more exactly, the inverse of the local vorticity). Since by assumption we’re taking the pure circulation case, the eddy produces zero change to the gas density. In Fig. 1, we initialize a simple grid of such eddies in two dimensions (though the results are essentially identical if we used three-dimensional Burgers vortices), and initialize a distribution of dust with randomly distributed initial positions and velocities (uniformly distributed), and evolve the system according to Eq. 1 for one  $t_e$  (the characteristic lifetime of eddies).

If  $t_s \gg t_e$ , grains with some random velocities will simply pass

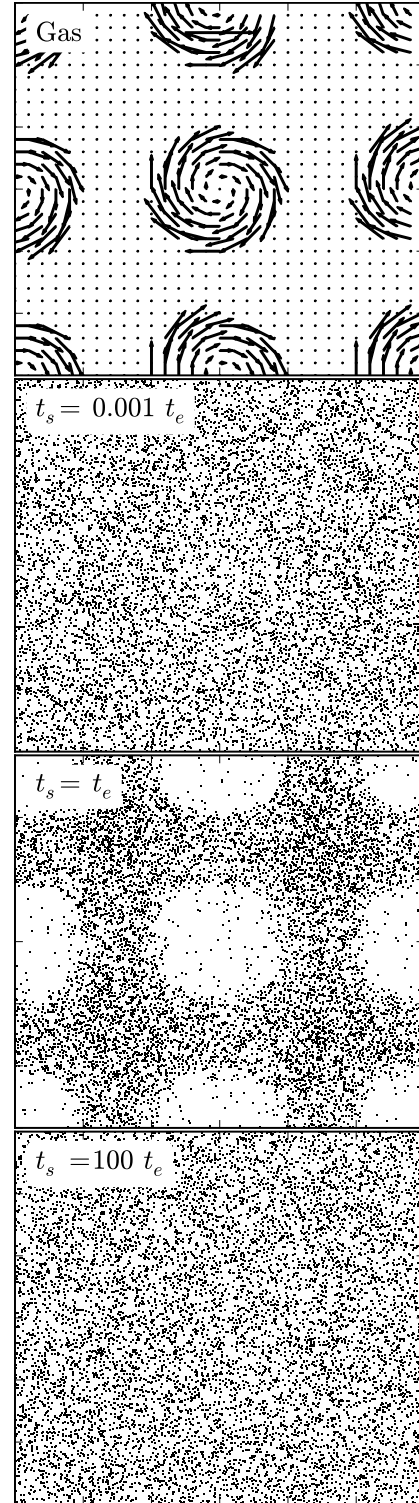


**Figure 1.** Illustration of the physics that drive dust-to-gas fluctuations in turbulence. We initialize  $10^4$  dust particles that move aerodynamically (Eq. 1), with random initial positions and velocities, and evolve them in a field of identical eddies for exactly one turnover time  $t_e$ . *Top:* Gas velocity field. We consider a periodic box with identical vortices (each with circulation velocity  $= r/t_e$  out to size  $r_0$ , and spaced in a grid, with no velocity in-between). The gas is in pure circulation so  $\nabla \cdot \mathbf{v} = 0$  everywhere (the gas density does not vary). *Bottom:* Positions of the particles after  $t_e$ , for different stopping times  $t_s = (0.001, 1, 100)t_e$ . If  $t_s \ll t_e$ , dust is tightly-coupled to the gas (it circulates but cannot develop density fluctuations). If  $t_s \gg t_e$ , dust does not “feel” the eddies, so moves collisionlessly. If  $t_s \sim t_e$ , dust is expelled from vortices and trapped in the interstices.

<sup>1</sup> The expression for  $t_s$  is for the Epstein limit. It is modified when  $a \gtrsim 9\lambda/4$ , where  $\lambda$  is the mean free path for molecular collisions, but this is never relevant for the parameter space we consider.

<sup>2</sup> This is true for both carbonaceous and silicate grains in detailed models such as those in Li & Draine (2001); Draine & Li (2007), but also follows trivially from the “canonical” power-law grain size spectrum  $dN/da \propto a^{-(3.0-3.5)}$ , giving  $dm/d\ln a \propto a^4 dN/da$  (Mathis et al. 1977).

<sup>3</sup> Note that the grain-grain collision time is always larger than  $t_s$  by a factor  $\gtrsim 1/Z_p$ , where  $Z_p$  is the grain mass fraction, so it is *not* what determines the grain dynamics.

through the eddy without being significantly perturbed by the local velocity field, so their density distribution is also unperturbed. If  $t_s \ll t_e$  is sufficiently small, the grains are efficiently dragged with the gas so cannot move very much *relative* to the gas in the eddy itself. But when  $t_s \sim t_e$ , interesting effects occur. The grains are partly accelerated up to the eddy rotational velocity  $v_\phi \sim u_e$ . But this means they feel a centrifugal acceleration  $\sim v_\phi^2/r$ . For the gas, this is balanced by pressure gradients, but the grains feel this only indirectly (via the drag force); so they get “flung outwards” until the outward drag  $\sim v_{\text{out}}/t_s$  balances centrifugal forces. Thus they “drift” out of the eddy at a terminal velocity  $v_{\text{out}} \sim t_s v_\phi^2/r \sim (t_s/t_e)u_e$ . Since eddies live for order  $\sim |t_e|$ , the grains initially distributed inside  $\sim r_e$  end up “flung out” to  $\sim (1 + t_s/t_e)r_e$ . When  $t_s \sim t_e$  this implies an order-unity median multiplicative change in the grain density *every time* the grains encounter a single turbulent eddy!

Indeed, in laboratory experiments, numerical simulations, and analytic theory (see Hopkins 2013b, and references therein), the full clustering statistics of dust grains in inertial-range turbulence depends only on the dimensionless parameter  $t_s/t_e(R)$ , the ratio of the gas friction time  $t_s$  to the eddy time  $t_e(R)$  as a function of scale  $R$  (since, in full turbulence, eddies of all sizes exist, but they have different vorticities on different scales). In an external gravitational field or shearing disk, additional corrections appear but these are also scale free (depending on e.g. the ratio  $t_s/t_{\text{orbit}}$ ). Generically, whenever  $t_s \sim t_e$ , grains are partially accelerated to be “flung out” of regions of high vorticity by centrifugal forces, and preferentially collect in the interstitial regions of high strain (Yoshimoto & Goto 2007; Bec et al. 2008; Wilkinson et al. 2010; Gustavsson et al. 2012). Properly integrating over many encounters per dynamical time, and encounters over various scales (eddies or modes of various sizes super-posed on one another in the turbulent cascade), order-of-magnitude fluctuations are easily produced (Hopkins 2013b); factors of  $\sim 100 - 10^4$  fluctuations are common in terrestrial turbulence and protoplanetary disks (Bai & Stone 2010a; Johansen et al. 2012).

Many authors have pointed out that the relevant phenomena are entirely scale free if these conditions are met (Cuzzi et al. 2001; Hogan & Cuzzi 2007; Bec et al. 2009; Olla 2010). In Hopkins (2013b) we derive rigorously the conditions for this to occur, as well as the width of the “resonance” region between timescales, and use this to build a model which reproduces the measured statistics of grain density fluctuations in both the simulations and laboratory experiments.

### 2.3 Generic PreConditions for Grain Density Fluctuations

Dust grains – or any aerodynamic particles – can undergo strong density fluctuations in gas provided three criteria are met:

(1): The medium is predominantly atomic/molecular. Specifically, exchange of free electrons, Coulomb interactions, and/or coupling of ionized dust grains to magnetic fields will couple the dust-gas fluids more strongly than aerodynamic drag when the ionized fraction exceeds some threshold of order a percent (for conditions considered in this paper;<sup>4</sup> for a rigorous calculation see Elmegreen 1979).<sup>5</sup> At the densities and temperatures of interest here (molecu-

lar cloud cores), typical ionization fractions are  $\lesssim 5 \times 10^{-8}$  (Guelin et al. 1977; Langer et al. 1978; Watson et al. 1978); so this criterion is easily satisfied.<sup>6</sup> We should note that under the right conditions, direct coupling between the grains and magnetic fields, or photo-electric coupling of grains and radiation, can actually *enhance* and generate new instabilities driving grain density fluctuations (Lyra & Kuchner 2013). But the behavior in these regimes is poorly understood.

(2): The medium is turbulent, with non-zero vorticity. There is no question that the ISM is turbulent under conditions we consider (with large Reynolds numbers). Within turbulence, the vorticity field (the solenoidal or  $\nabla \times \mathbf{v}$  component) of the gas is what drives large grain density fluctuations independent of gas density fluctuations. The governing equations for grain density fluctuations over the inertial range (see Zaichik & Alipchenkov 2009) are independent of both whether or not the turbulence is super-sonic or sub-sonic, and whether the gas is compressible, except insofar as these change the ratio of solenoidal to compressive motions (essentially just re-normalizing the portion of the turbulent power spectrum that is of interest). In highly sub-sonic, incompressible flows, all of the turbulent power is in solenoidal motions; but even in highly compressible, isothermal, strongly super-sonic turbulence *driven* by purely compressive motions, the cascade (below the driving scale) quickly equilibrates with  $\approx 2/3$  of the power in solenoidal motions (this arises purely from geometric considerations; see Federath et al. 2008; Konstantin et al. 2012). Thus up to a normalization of  $2/3$  in the driving-scale rms velocity field, this is easily satisfied.

(3): There is a resonance between the grain stopping time  $t_s$  and turbulent eddy turnover time  $t_e$ :  $t_s \sim t_e$ . We discuss this below.

### 2.4 Specific Requirements in Molecular Clouds

Provided condition (1) is met, a grain obeys the Stokes equations (Eq. 1). Now consider a molecular cloud which is supersonically turbulent with mass  $M_{\text{cl}}$ , size  $R_{\text{cl}} = 10 R_{10}$  pc, surface density  $\Sigma_{\text{cl}} = M_{\text{cl}}/(\pi R_{\text{cl}}^2) = \Sigma_{300} 300 M_\odot \text{pc}^{-2}$ , and sound speed  $c_s \approx 0.2 T_{10}^{1/2} \text{km s}^{-1}$  ( $T_{10} = T/10 \text{K}$  is the cold gas temperature, and we take a molecular weight  $\approx 2$  appropriate for a solar mixture), and cloud-scale rms turbulent velocity  $v_{\text{cl}} = \langle v_r^2(R_{\text{cl}}) \rangle^{1/2}$ . For a constant-mean density spherical cloud, the Toomre  $Q$  parameter is  $Q \approx (2/\sqrt{3}) v_{\text{cl}} \Omega / (\pi G \Sigma_{\text{cl}})$  with  $\Omega = \sqrt{GM_{\text{cl}}/R_{\text{cl}}^3}$ , and we expect  $Q \sim 1$  (even for a cloud in free-fall, this applies to within a factor  $\sim 2$ ). In a turbulent cascade, the rms velocity on a given scale

between neutral and charge  $Z_{\text{grain}} \sim -1$  for an assumed “sticking factor”  $s = 1$  (probability that grain-electron collision leads to capture); but  $s$  and other details are highly uncertain (Draine & Sutin 1987). If we assume that all grains spend most of their time charged, the relative importance of magnetic fields is given by the ratio of  $t_s$  to the Larmor period  $t_L = 2\pi m_{\text{grain}} c / (Z_{\text{grain}} e |B|)$ , which is  $t_s/t_L \approx 10^{-4} B_{\mu\text{G}} Z_{\text{grain}} a_\mu^{-2} n_{100}^{-1} \delta v_{\text{km s}^{-1}}$  (where  $B_{\mu\text{G}} = |B|/\mu\text{G}$ ,  $n_{100} = \langle n_{\text{gas}} \rangle / 100 \text{cm}^{-3}$ , and  $\delta v_{\text{km s}^{-1}}$  is the typical dust-gas relative velocity (between  $\sim c_s$  and  $\sim (c_s^2 + v_{\text{turb}}^2)^{1/2}$ , depending on scale). We can also write this as  $t_s/t_L \sim 0.01 Z_{\text{grain}} n_{100}^{-1/2} a_\mu^{-2} (|B|/|B_{\text{eq}}|)^{1/2}$  where  $|B|/B_{\text{eq}} = v_A^2/\delta v^2$  is the ratio of  $|B|$  to an equipartition value. So we generally expect  $t_s \ll t_L$  even for the case where all grains are (weakly) charged, in which case we can neglect the magnetic acceleration in calculating the response of grains to small-scale eddies. However, within plausible parameter space, the two effects can be comparable; in this limit the instabilities we describe have not been well studied.

<sup>6</sup> Provided this is satisfied, magnetic fields, even super-critical, do not alter our conclusions. In fact Dittrich et al. (2013) show that pressure waves and turbulence seeded by the fields in this limit actually enhance dust density fluctuations.

<sup>4</sup> Note that we are explicitly interested in large grains here with sizes  $\sim \mu\text{m}$ . PAHs and other very small grains (sizes  $\sim \text{\AA}$ ) are photo-electrically coupled differently (and much more strongly) to the radiation field (see e.g. Wolfire et al. 1995, and references therein).

<sup>5</sup> The case of grain coupling to magnetic fields is more complicated. For the conditions and grain sizes of interest here, grains are expected to vary

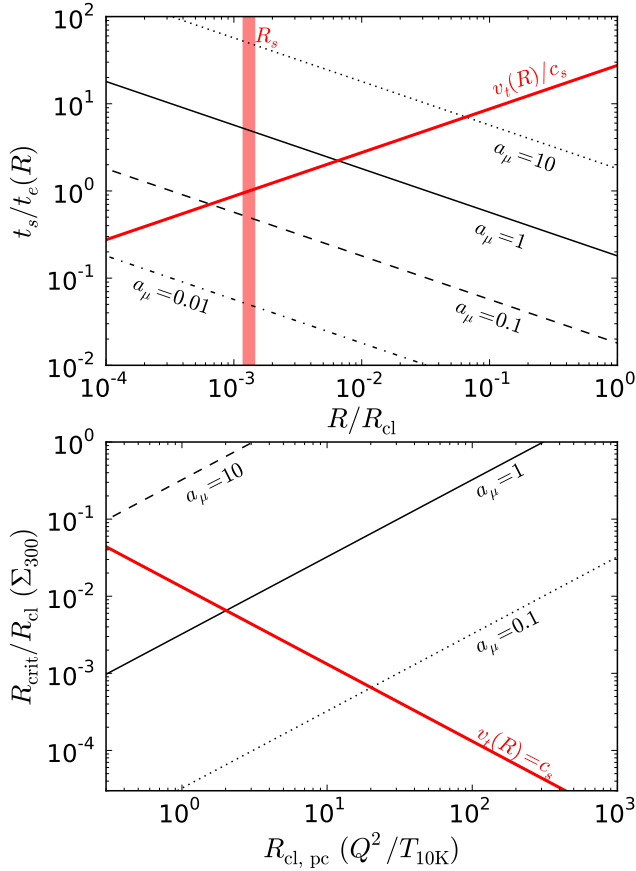


**Figure 2.** Conditions for strong dust-to-gas fluctuations in molecular clouds. *Top:* Ratio of grain stopping time  $t_s$  to eddy turnover time  $t_e$  for eddies of size  $R$ , relative to the cloud size  $R_{cl}$  (for a cloud with  $Q = 1$ ,  $\Sigma_{cl} = 300 M_{\odot} \text{pc}^{-2}$ ,  $T_{min} = 10 \text{ K}$ , and  $R_{cl} = 10 \text{ pc}$ ). Different curves assume different grain sizes  $a_{\mu}$ . Thick red curve shows the ratio of the rms turbulent eddy velocity  $v_t(R)$  to the sound speed; the scale where this = 1 (the sonic length  $R_s$ ) is the characteristic scale of cores. Small grains have  $t_s \ll t_e(R)$  for all  $R \gtrsim R_s$ ; but large grains cluster on larger scales. *Bottom:* Scale  $R_{crit}$  where  $t_s = t_e(R)$  (normalized to the cloud size), for different grain sizes (lines as labeled), as a function of the cloud size in pc. Red line shows the sonic length in clouds of the same size: where the black lines exceed the red line, core-to-core dust-to-gas ratio variations are expected.

follows  $\langle v_t^2(R) \rangle^{1/2} \propto R^p$  with  $p \approx 1/2$  expected for super-sonic turbulence and observed in the linewidth-size relation (Burgers 1973; Bolatto et al. 2008; Heyer et al. 2009). So the rms eddy turnover time on a given scale is  $t_e \equiv R / \langle v_t^2(R) \rangle^{1/2} = (R_{cl} / v_{cl}) (R / R_{cl})^{1/2}$ .

We then have

$$\left\langle \frac{t_s}{t_e(R)} \right\rangle = \sqrt{3\pi} Q \frac{G \bar{\rho}_{solid} a}{c_s \Omega} \left( \frac{R}{R_{cl}} \right)^{-1/2} \quad (3)$$

$$\approx 0.18 Q a_{\mu} \left( \frac{R_{10}}{\Sigma_{300} T_{10}} \right)^{1/2} \left( \frac{R}{R_{cl}} \right)^{-1/2} \quad (4)$$

We plot this in Fig. 2, for different grain sizes (and clouds with the characteristic parameters above). We compare the Mach number versus scale ( $\langle v_t^2(R) \rangle^{1/2} / c_s$ ), which we discuss below.

Note that even at the cloud-scale ( $R = R_{cl}$ ),  $t_s \sim 0.18 t_e(R_{cl}) = 0.18 \Omega^{-1}$  is sufficient to produce significant grain density variations (see Johansen & Youdin 2007; Bai & Stone 2010c; Dittich et al. 2013). However, the fluctuations are maximized on the scale  $R_{crit}$

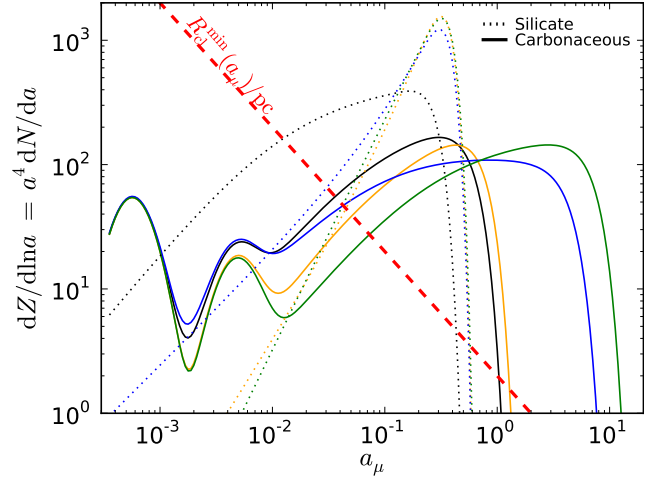


**Figure 3.** Size distribution of grains affected by turbulent clustering. We show the distribution of grain mass per log-interval in grain size  $a_{\mu}$  for carbonaceous (solid) and silicate (dotted) grains in several of the best-fit Weingartner & Draine (2001) models (the normalization is arbitrary, what matters here is the relative distribution in each curve). Different fits (or fits to different MW regions) give quite different results for the abundance of large grains, emphasizing their uncertain chemistry, but in all cases most of the mass is in large grains with sizes  $a_{\mu} \sim 0.1 - 10$ . Red dashed line shows the critical cloud size  $R_{crit}(a_{\mu})$  (above which grain density fluctuations are on super-core scales), for comparison. For a given cloud size, grains to the right of the corresponding  $a_{\mu}$  on the plot will experience core-to-core density fluctuations.

where  $\langle t_s \rangle = \langle t_e(R_{crit}) \rangle$ , so we can solve for the characteristic scale

$$R_{crit} = R(\langle t_s \rangle = \langle t_e \rangle) = 0.31 \text{ pc} \frac{a_{\mu}^2 Q^2 R_{10}^2}{\Sigma_{300} T_{10}} \quad (5)$$

In the lower panel of Fig. 2, we show this critical scale versus cloud size, again for different grain sizes.

If this scale ( $R_{crit}$ ) is much less than the characteristic scale of the regions which collapse into pre-stellar cores ( $R_{core}$ ), then many independent small fluctuations will ultimately collapse into the same object (or stellar multiple) and be mixed, “averaging out” and imprinting little net abundance fluctuation in the stars (although they may seed interesting metallicity variations in the proto-stellar disk). However if  $R_{crit} \gtrsim R_{core}$ , then independent collapsing regions will have different grain densities. A wide range of both simulations and analytic calculations show that  $R_{core}$  is characteristically the sonic length  $R_s$ , the size scale below which the turbulence is sub-sonic ( $\langle v_t^2(R < R_s) \rangle < c_s^2$ ; see Klessen & Burkert 2000, 2001; Bate & Bonnell 2005; Krumholz & McKee 2005; Hennebelle & Chabrier 2008; Hopkins 2012c,b, 2013c). We show this scale for comparison in Fig. 2. Below this scale, turbulence can no longer drive significant density fluctuations, so collapse proceeds semi-coherently (as opposed to a turbulent fragmentation cascade). For the cascade above,  $R_s = R_{cl} (c_s / v_{cl})^2$ , so

$$\frac{R_{crit}}{R_s} = 23.5 \left( \frac{a_{\mu} R_{10} Q^2}{T_{10}} \right)^2 \quad (6)$$

Seeding large fluctuations in cores ( $R_{crit} > R_s$ ) therefore requires

$$R_{cl} \gtrsim \frac{2}{3\pi Q^2} \frac{c_s^2}{G \bar{\rho}_{solid} a} \quad (7)$$

$$R_{10} \gtrsim 0.2 a_{\mu}^{-1} Q^{-2} T_{10} \quad (8)$$

or (equivalently)

$$M_{cl} \gtrsim 0.4 a_{\mu}^{-2} \times 10^4 M_{\odot} \Sigma_{300} T_{10}^2 Q^{-4} \quad (9)$$

Note this is a cloud mass, not a cluster mass! The model here does not necessarily predict a cluster stellar mass threshold (which depends on the star formation efficiency), but a progenitor cloud mass threshold.

## 2.5 Resulting Dust-to-Gas Density Fluctuations

Under these conditions, the density of grains averaged on scales  $\sim R_{\text{crit}}$  will undergo large turbulent concentration fluctuations (fluctuations driven by local centrifugal forces in non-zero vorticity). Since this depends on the *vorticity* field, which is the incompressible/solenoidal component of the turbulence, this component of the fluctuations is entirely independent of gas density fluctuations (driven by the compressive field components).<sup>7</sup> Thus we expect large fluctuations in the dust-to-gas mass ratio  $Z_p \equiv \rho_p/\rho_g$ . Specifically, only grains with sufficiently large  $a_\mu$  such that the condition in Eq. 8 is satisfied are inhomogeneous on the relevant scales. In Fig. 3, we plot the distribution of grain mass as a function of grain size  $a_\mu$ , from various fits of observations presented in Weingartner & Draine (2001); for comparison we show the critical cloud size  $R_{\text{cl}}$  where large core-to-core variations are expected at each  $a_\mu$ . Although there are significant differences between different model fits, and different types of grains (silicate vs. carbonaceous), clearly grains with  $a_\mu \sim 1$  contain most of the dust mass, and, correspondingly, an order-unity fraction of the total metal mass, so large  $Z_p$  fluctuations translate directly to large  $Z$  variations in the appropriate species.

Hopkins (2013b) show that, for systems with this range of  $t_s \Omega$  and  $t_s/t_e$ , the volume-weighted variance in the logarithm of the dust-to-gas density  $\ln Z_p$  is given by<sup>8</sup>

$$S_{\ln Z_p} = \int_{R_{\min} \sim R_s}^{R_{\max} \sim R_{\text{cl}}} 2 |\mathfrak{W}(R/R_{\text{crit}})|^2 d \ln R \quad (10)$$

$$\sim 4.9 - 8 \left( \frac{R_{\text{crit}}}{R_{\text{cl}}} - \sqrt{\frac{R_s}{R_{\text{crit}}}} \right) \quad (11)$$

where the latter assumes  $R_{\text{cl}} \gg R_{\text{crit}} \gg R_s$ ; so for typical parameters the  $1\sigma$  dispersion in metallicities is  $\sim 1$  dex. Indeed, this can be directly compared to simulations in Johansen & Youdin (2007) and Dittrich et al. (2013) which have  $t_s \Omega \sim 0.1$  and otherwise similar (dimensionless) parameters to those calculated here; this predicts a similar  $\sim 1$  dex variance.<sup>9</sup>

<sup>7</sup> There will, of course, be a component of the grain density fluctuations which traces advection through the compressive component of the turbulent field. This is not interesting for our purposes here, however, since the gas does the same so it imprints no variation in the gas-to-dust ratio.

<sup>8</sup> Here  $\mathfrak{W}(R/R_{\text{crit}})$  is the “response function” – the logarithmic density change per eddy turnover time induced by encounters between grains and an eddy with some  $t_e$  – in general it is a complicated function given in Table 1 therein, but it only depends on the dimensionless ratios  $t_s/t_e(R)$  and  $t_s \Omega$ , and scales simply as  $\approx (t_s/t_e)$  when  $t_s \ll t_e$  and  $\approx 1/\sqrt{2(t_s/t_e)}$  when  $t_s \gg t_e$  (with a broad peak where  $\mathfrak{W} \approx 0.3$  around  $t_s \approx t_e$ ).

<sup>9</sup> For the same  $t_s/t_e$  and  $t_s \Omega$  simulated in Johansen & Youdin (2007); Bai & Stone (2010b), the only parameter which affects the dust density distributions simulated, or enters the analytic calculation of those density distributions in Hopkins (2013b), and may differ between the proto-planetary disk problem studied therein and the molecular cloud case is the  $\beta \propto 1/\Pi$  parameter which depends on the cloud/disk-scale Mach number and gas pressure support. In the highly super-sonic limit,  $\beta \rightarrow \infty$ . But the effect of this in the simulations is simply to take to zero the small-scale “cutoff” below which the contribution of turbulent eddies to the grain clustering is damped; thus if anything the “real” clustering in the molecular cloud case should be slightly larger than in those simulations.

Thus, the cloud is “seeded” with not just gas-density fluctuations (which form cores and determine where stars will form), but independent dust-to-gas ratio fluctuations, which are then “trapped” if they are associated with a collapsing core, so that the abundance in that core, and presumably the star formed, will be different. Note that if the conditions above are met, the characteristic timescale for the density fluctuations to disperse is always  $\sim t_e(R_{\text{crit}})$ . But by definition, for a region to collapse as a core, and overcome turbulent kinetic energy as well as shear and pressure terms to become a star, its collapse time must be shorter than  $t_e$  (see Hennebelle & Chabrier 2008; Padoan & Nordlund 2011; Hopkins 2013a), so the fluctuations are “frozen into” the cores.<sup>10</sup>

Laboratory experiments (Monchaux et al. 2010), simulations (Hogan et al. 1999; Cuzzi et al. 2001), and the analytic models (Hopkins 2012a) show these dust density fluctuations have a characteristically log-Poisson shape:

$$P_V(\ln Z_p) d \ln Z_p \approx \frac{\Delta N_{\text{int}}^m \exp(-\Delta N_{\text{int}})}{\Gamma(m+1)} \frac{d \ln Z_p}{\Delta} \quad (12)$$

$$m = \Delta^{-1} \left\{ \Delta N_{\text{int}} \left[ 1 - \exp(-\Delta) \right] - \ln \left( \frac{Z_p}{\langle Z_p \rangle} \right) \right\}$$

where  $\Delta N_{\text{int}} \sim 2 \langle \ln(R_{\text{cl}}/R_{\text{crit}}) \rangle$  traces the dynamic range of scales which can contribute to grain density fluctuations, and  $\Delta = \sqrt{S_{\ln Z_p}/\Delta N_{\text{int}}}$  is the rms weighted dispersion induced “per eddy” around  $\sim R_{\text{crit}}$ . In the limit where  $N_{\text{int}} \gg 1$  (and to leading order around the mean  $Z_p$ ), this distribution is just log-normal. The mass-weighted distribution  $P_M$  is just given by  $P_M = Z_p P_V$  (also approximately log-normal, with the same variance).

However, although this distribution extends to  $Z_p \rightarrow 0$ , the actual metallicities  $Z$  imprinted on the cores do not. The minimum  $Z$  in a core will be given by the sum of the metals in a non-condensed phase (not in dust) and those in grains so small that their clustering scale is well below  $R_s$ . In the Weingartner & Draine (2001) models, the sum of non-condensed metals and grains with  $a_\mu < 0.1$  is  $1 - f_p \sim 30 - 60\%$  of the total metal mass; so while large positive abundance enhancements may be possible, the largest decrements will be factor of a few. More generally, if for some species the mean mass fraction in large grains is  $\langle Z_p \rangle = f_p \langle Z \rangle$ , then the abundance of a given core will be  $Z_c/Z = (1 - f_p) + f_p \langle Z_p \rangle / \langle Z \rangle$ ; so the variance in  $Z$  imprinted on cores is reduced with  $f_p$ . To first order, this is just

$$S_{\ln Z_c} \approx f_p^2 S_{\ln Z_p} \quad (13)$$

Also from Hopkins (2013b), the maximum fluctuation amplitude we expect is given by

$$\ln \left( \frac{Z_p^{\max}}{\langle Z_p \rangle} \right) \approx 2 \int_{R_s}^{R_{\text{cl}}} [1 - \exp(-2\mathfrak{W})] d \ln R \quad (14)$$

$$\sim 9.7 \exp[-1.12(R_s/R_{\text{crit}})^{1/4}] \sim 4.5 - 5.5 \quad (15)$$

where the latter assumes  $R_{\text{cl}} \gtrsim 100 R_{\text{crit}}$  (though this enters weakly). Thus we can obtain  $Z_p^{\max} \sim 100 \langle Z_p \rangle$ . This also agrees well with simulations of the similar parameter space; and although it seems large, it is actually much smaller than the largest fluctuations which can be obtained under “ideal” circumstances ( $t_s \Omega \approx 1$ , where  $Z_p^{\max} \sim 10^4 \langle Z_p \rangle$  is possible; see Bai & Stone 2010a; Johansen et al. 2012). Comparing to the simulations or simply plugging in

<sup>10</sup> It is also worth noting that these characteristic timescales (at the spatial scales of interest), and the timescale for “seeding” the density fluctuations ( $\sim t_s$ ) are much shorter than the timescale for e.g. grain drift/segregation by radiation pressure or grain formation/destruction, so we can reasonably ignore those effects.

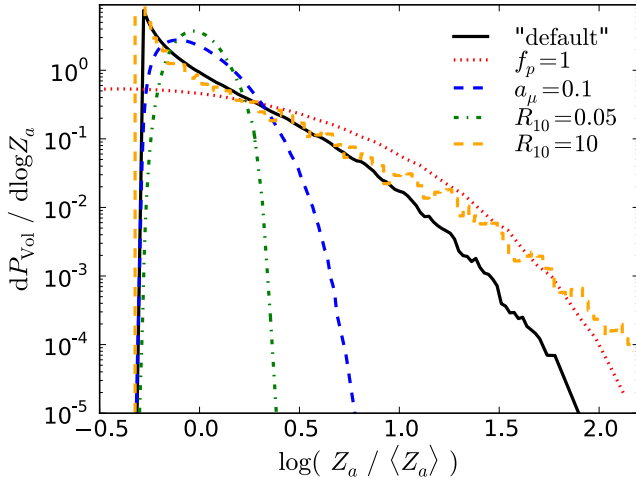


**Figure 4.** Predicted volumetric distribution of the metallicity fluctuations ( $Z_a$ , relative to the cloud-mean  $\langle Z_a \rangle$ ) seeded by grain density fluctuations. In the “default” case, we assume that a fraction  $f_p = 0.5$  of the metal species of interest is condensed into grains with size  $\geq a_\mu = 1$ , in a cloud with  $R_{10} = T_{10} = \Sigma_{300} = 1$ . Since  $1 - f_p = 1/2$  of the metallicity is in small grains and/or gas, it imposes a hard cutoff at low- $Z_a$ , but positive fluctuations extend to large values  $\sim 30 \langle Z_a \rangle$ . We then consider the same case but with all metals in large grains ( $f_p = 1$ ; red dotted); this extends the large- $Z_a$  by a factor  $1/f_p$ , and leads to a predicted low- $Z_a$  tail. We also compare a case identical to our “default” but with smaller grains  $a_\mu = 0.1$  (blue dashed) or a much smaller cloud ( $R_{10} = 0.05$ ; green dot-dashed); here the resulting fluctuations are much smaller (factor  $< 2$ ). Finally we consider the “default” case but with  $R_{10} = 10$  (a 100 pc cloud; orange dashed); now the largest positive fluctuations extend to factors of  $\sim 100$  – the resulting cores would actually be *predominantly* metals by mass!

this value to the log-Poisson distribution above, we see that the *mass* fraction associated with such strong fluctuations is small,  $\sim 10^{-4} - 10^{-3}$ . However, these would be extremely interesting objects; if the seed  $\langle Z_p \rangle \sim Z_\odot \sim 0.01 - 0.02$ , then in these rare collapsing cores,  $Z_p \gtrsim 1$  – i.e. the collapsing core is *primarily* metals!

In Fig. 4, we calculate the full PDF of grain density fluctuations, integrating the contribution from the “response function” from the top scale  $R_{cl}$  down to the core scale  $R_s$ , according to the exact functions derived and fit to simulation data in Hopkins (2013b). This confirms our simple (approximate) expectations above. We assume a fraction  $f_p$  of the metals are concentrated in grains, which (by assumption) imprints a cutoff in the negative metal density fluctuations at  $1 - f_p$ . But the positive-fluctuation distribution is log-Poisson (approximately log-normal), and extends to larger values of  $S_{ln Z_p}$  as the ratio of  $R_{crit}/R_s$  increases (i.e. with larger clouds and/or grain sizes). The largest positive fluctuations are predicted reach  $Z \sim 30 - 300 \langle Z \rangle$ , depending on the detailed conditions, with a fractional probability by volume (i.e. probability that a random location has such a strong fluctuation) of  $\sim 10^{-3} - 10^{-4}$ .

### 3 PREDICTIONS

This makes a number of unique predictions:

(1) Stars formed in small clouds are not affected (chemically homogeneous). The key requirement is that the size of the progenitor GMC exceed  $R_{cl} \gtrsim 2 \text{ pc } Q^{-2} (T_{min}/10 \text{ K}) a_\mu^{-1}$ , where  $a_\mu$  is the grain size which contains most of the metal mass ( $\sim 0.1 - 1$ , depending on the species). This corresponds to a GMC mass  $\gtrsim 10^4 a_\mu^{-2} M_\odot$ , for typical cloud densities in the local group.

(2) Larger/more massive clouds can experience large dust-to-gas ratio (hence, abundance) fluctuations from core-to-core. The

rms fluctuations could reach as large as  $\sim 1$  dex under the right conditions. And these fluctuations should be “frozen into” the cores that collapse under self-gravity, meaning they will manifest in the stars formed from those cores.

(3) These dust density fluctuations will *not* obviously manifest as variation in the dust extinction. While most dust mass (or volume) is in large grains ( $a_\mu \sim 0.1 - 1$ ), most of the surface area (hence contribution to extinction in most wavelengths) is in small grains ( $a_\mu < 10^{-3}$ ; the small “bump” in Fig. 3). The small grains cluster only on scales  $\sim 10^6$  times smaller (sub-au), so trace the gas smoothly on core and GMC scales. Only dust features which are specifically sensitive to large grains will exhibit large spatial-scale fluctuations. Sub-mm observations, and other long-wavelength probes, may be sensitive to some of the features of larger dust, and so represent a way forward to constrain this process directly.

(4) Because it is large grains that are preferentially clustered, certain metal species are preferentially affected. Inverting Eq. 8, we see that the minimum grain size which will be highly clustered on the relevant scales goes as  $a_\mu \sim 0.2 T_{10} R_{10}^{-1} \sim 1.6 (M_{cl}/10^4 M_\odot)^{-1/2} \Sigma_{300}^{-1/2} T_{10}$ .

Carbon and other light elements (C, O), concentrated in large composite grains and ices forming on the grains under GMC conditions ( $a_\mu \sim 1 - 20$  in Fig. 3; see e.g. Hoppe & Zinner 2000), will exhibit the largest fluctuations, and these fluctuations will appear “first” in lower-mass clusters ( $M_{cl} \gtrsim 10^4 - 10^5 M_\odot$ ).<sup>11</sup> Slightly heavier species (Al) will follow in clusters  $\gtrsim 10^5 M_\odot$ . Heavier elements typical of Type-II SNe products and iron-peak elements (Ca, Fe) are largely concentrated in small carbonates and oxides, with  $a_\mu \lesssim 0.1$  – these abundances will only fluctuate in the most extreme clouds with masses  $M_{cl} \gtrsim 10^7 M_\odot$ . Si ( $a_\mu \sim 0.2 - 0.4$ ; see Fig. 3) will be intermediate between these and Al.

(5) Very light elements such as Li, or chemically inert elements such as He and Ne, not being concentrated in grains, will not vary in abundance by this mechanism. In contrast, most models for abundance variation via self-enrichment (from mass loss products) or stellar evolution predict large He and Li variation. This gives a clear diagnostic to separate these processes. Some clusters certainly exhibit large He spreads (Piotto et al. 2007), but others show surprisingly small He and Li spreads, despite other abundance variations (Monaco et al. 2012).

(6) The *shape* of the distribution of abundances seeded by turbulent concentration is approximately log-normal, or more accurately log-Poisson. This is consistent with some observed clusters, and may provide another way to separate variations owing to this process from self-enrichment processes which predict a more bi-modal distribution (see Carretta et al. 2009b,a, 2013). The process seeding the variations (turbulent concentration) is also stochastic, which means that there is intrinsic cluster-to-cluster variation (even at the same initial mass and abundance).

(7) Large negative abundance variations will not occur, because cores will still retain a minimum metallicity corresponding to the metals in non-condensed phases and very small grains. Thus the abundance distribution will be truncated at a minimum of a factor a couple below mean.

(8) At higher cloud surface densities ( $\Sigma$ ) and/or minimum gas

<sup>11</sup> N may be an interesting case, since while it is probably concentrated in organic refractories in the largest grains (Zubko et al. 2004), it is mostly in gas-phase, so the variance may be smaller by a factor of  $\sim 4 - 8$  than in C or O.

temperatures ( $T$ ), the cloud mass threshold required for these variations increases. Both  $\Sigma$  and  $T$  do appear to increase with the overall gas density and star formation rate density – for example in the nuclei of ultra-luminous infrared galaxies/starbursts and high-redshift galaxies. For typical ULIRG-like conditions,  $Q \sim 1$  remains constant, but  $T_{10} \sim 5-7$  and  $\Sigma_{300} \sim 10-30$  – so this process requires  $R_{10} \gtrsim 1 a_{\mu}^{-1}$  or  $M_{cl} \gtrsim 10^6 a_{\mu}^{-2} M_{\odot}$ . However, the characteristic Jeans length/mass also increases under these conditions (for a detailed comparison, see Hopkins 2012c), up to several hundred pc (and  $\gtrsim 10^8 M_{\odot}$ ); the thermal Jeans length/mass increases more rapidly with temperature than the critical cloud radius, for example. So whether older clusters exhibit weaker or stronger abundance variations will depend on the types of galaxies in which they formed, in detail, but we generically expect this process to be easier in the early Universe and extreme environments.

(9) Unlike abundance variation stemming from stellar evolution, binary effects, pollution, or second-generation star formation, the variations predicted here are imprinted *before* stars form and evolve, and so are independent of whether or not the final cluster remains bound. Thus we predict similar trends in open clusters (OCs) and associations (not just bound clusters).

(10) A small sub-population of proto-stellar cores (one in  $\sim 10^3 - 10^4$ ) is predicted with metallicities  $Z_p \gtrsim 100 \langle Z_p \rangle$ . If the initial cloud metallicity is solar ( $Z_p \gtrsim 0.01$ ), this implies  $Z_p \sim 1$  – cores would collapse into stars which are almost “totally metal”!

The collapse process of such cores is not entirely clear, since it depends on the behavior of grains in the collapsing cloud. If the grains can stick efficiently, they will grow to large sizes, forming a self-gravitating cloud of pebbles. The cloud would thus go through an intermediate or adolescent “rock” phase before progressing to its more mature “metal-star” phase. More likely, the grains will shatter as the cloud collapses (since their collision velocities would be comparable to the gravitational free-fall velocity, hence large). This would reduce them to small grains and gas-phase metals, enhancing the cloud cooling, thus further promoting rapid collapse, until the cloud forms a star.

The massive versions of such metal stars would burn through their light elements quickly (much faster than their less-metal rich counterparts). They may not appear very different from other massive stars which have already depleted their light elements (although the opacities in the earlier stages would be very different). But low and intermediate-mass stars formed in this fashion would be longer-lived, and very unusual. Being so metal rich, they would likely be quite compact, and as a result appear as anomalously hot, blue populations, with unusually small hydrogen envelopes. But this fundamentally represents a novel stellar evolution channel, one which has not yet been well-explored.

## 4 RELEVANCE TO OBSERVED STAR CLUSTERS AND GALAXIES: DOES THIS MATTER?

### 4.1 Carbon-Enhanced Stars

The most natural result of the process described here is a population of stars enhanced specifically in the elements associated with the largest grains: C in particular (since these are carbonaceous grains; the largest often graphite chains). It has long been known that there are various populations of anomalously carbon-rich stars (see e.g. Shane 1928); more recently, large populations of carbon-enhanced metal-poor stars (CEMPS) have been identified with  $[C/Fe] \sim 0-4$ .

Among the “normal metallicity” carbon-rich population, many features follow naturally from the predictions here. They have high  $[C/Fe]$ , but also usually have  $[C/O] > 1$  – this is highly

non-trivial, since while  $[C/O] > 1$  is generically true inside a carbonaceous grain, it holds almost nowhere else in the Universe. Among the carbon-rich population, the “early-R” sub-population (which constitutes a large fraction of all carbon-rich stars; Blanco 1965; Stephenson 1973; Bergeat et al. 2002a) has properties which most naturally follow from this scenario: enhanced C, but no enhancement in s-process elements, little Li enhancement, and an absence of obvious companion or merger signatures (Dominy 1984; McClure 1997; Knapp et al. 2001; Zamora et al. 2009, and references therein). Given the relatively modest C enhancements needed ( $\sim 0-1$  dex), their abundance by number (a few to tens of percent of the carbon-star population), locations in both the thick and thin disk, and broad mass distribution are also all easily consistent with our proposed scenario (Bergeat et al. 2002b). And the unusual isotopic ratios observed in  $^{12}C/^{13}C$  ( $\lesssim 10-20$ ) are almost identical in their distribution to those directly observed in presolar carbide grains (for a review, see Zinner 2014 and The Presolar Grain Database, Hynes & Gyngard 2009) – it will be very interesting to see if the same holds for other measured isotopic ratios in grains (such as  $^{14}N/^{15}N$  or  $^{17,18}O/^{16}O$ ). Moreover, alternative explanations for this sub-population, including stellar evolution processes (mixing or production from rotation, convection, unusual AGB phases or He-flashes), stellar mergers or mass transfer, all appear to make predictions in serious conflict with the observations (Izzard et al. 2007; Zamora et al. 2009; Mocák et al. 2009; Piersanti et al. 2010). These stars could simply be “primordially” enhanced in the species most abundant in large grains. They may also represent the sites of new grain formation, in which case the connection would be self-reinforcing over multiple generations of star formation!

On the other hand, while grain density fluctuations may play a role in seeding some C abundance variations in the “N” and “J” sub-populations of carbon stars, these exhibit features such as enhanced Li, s-process products, and  $^{13}C$  abundances which are not obviously predicted by this process (and indeed, AGB mixing, mass loss, and merger process appear to explain them; Abia & Isern 2000; Abia et al. 2002; Zhang & Jeffery 2013).

In an environment with very low mean metallicity but large fluctuations in  $[C/H]$  owing to large grain density inhomogeneities, CEMPS would be especially favored to form, because the regions with enhanced dust density would be the ones that could easily cool and thus actually form stars, whereas regions with low  $[C/H] \lesssim -3$  generically have cooling times much longer than their dynamical times and so cannot efficiently form stars (see e.g. Barkana & Loeb 2001, and references therein). Our calculations here have generally focused on conditions closer to solar mean metallicity where cooling is always efficient, so in a future paper we will consider in more detail the specific predictions for CEMPS owing to the interplay between dust density fluctuations and cooling physics.

### 4.2 Globular Clusters

This mechanism may explain some of the observed star-to-star abundance variations in massive globular clusters (Carretta et al. 2009b), and would resolve some tension between observations of abundance spreads and constraints on second-generation star formation (Muno et al. 2006; Sana et al. 2010; Seale et al. 2012; Bastian et al. 2013a; Larsen et al. 2012). However, we wish to emphasize that we do not expect this scenario to provide a complete description of abundance variations in massive GCs. Enhanced He, and a tight anti-correlation between Na and O, are not obviously predicted by grain clustering. Indeed, other processes such as pollution by stellar mass-loss products, second-generation star formation, and complicated multiple interactions certainly occur, and



probably dominate the observed variation in these systems (see e.g. D’Ercole et al. 2008; Conroy & Spergel 2011; Bastian et al. 2013b).

### 4.3 Open Clusters

As noted in § 3 point (9) above, unlike the second-generation products invoked in GCs, we expect this process to occur identically in sufficiently massive open clusters. Measuring abundance spreads in open cluster stars is challenging and very few open clusters (especially very massive ones) have strong constraints (see Martell & Smith 2009; Pancino et al. 2010; Bragaglia et al. 2012; Carrera & Martinez-Vazquez 2013). In the (limited) compilations above, every OC for which significant abundance spreads can be definitively ruled out lies significantly below the threshold size/mass (1) we predict. Interestingly, the couple marginal cases (NGC 7789, Tombaugh 2) lie near the threshold, but with large systematic uncertainties in these quantities (Frinchaboy et al. 2008).

One currently known OC (NGC 6791) definitely exhibits abundance spreads (Carraro 2013, and references therein). Interestingly, many apparently “anomalous” properties of this cluster may fit naturally into our scenario. The spreads in Na and O are very large,  $\sim 0.7$  dex (and may be multi-modal; Geisler et al. 2012); with little spread in Fe. Particularly striking, Na and O are *not* anti-correlated, as they are in models where the abundance variations stem from stellar evolution products. The absolute metallicity is also very high ( $[\text{Fe}/\text{H}] \sim 0.4 - 0.5$ ), suggesting a high dust-to-gas ratio which would make the effects described here both stronger and more directly observable (since the condensed-phase heavy element abundances should be larger). It is one of the most massive open clusters known, with mass of a few  $\times 10^4 M_\odot$  and size  $\gtrsim 20$  pc, making it one of the only OCs above the threshold predicted (Carrera 2012). And it appears to exhibit an anomalous blue horizontal branch stellar population; this has many degenerate explanations but may be the product of highly metal-enhanced stars with relatively small, quickly-depleted hydrogen envelopes (see e.g. Liebert et al. 1994; Twarog et al. 2011; Carraro 2013).

### 4.4 The UV Excess in Elliptical Galaxies

It is well-known that early-type galaxies exhibit an anomalous “UV excess” (UVX) or “UV upturn” – an excess of UV light stemming from old stellar populations, generally attributed to a “hot” (excessively blue) population of “failed AGB” or “slow blue” post-horizontal branch phases of stars which are metal-rich and have relatively small light-element envelope masses (for reviews, see e.g. Horch et al. 1992; Greggio & Renzini 1999).

Interestingly, the UVX appears to be empirically identical to the excess population seen in NGC 6791 – if a couple percent of the luminosity of ellipticals were composed of stellar populations identical to NGC 6791, the integrated light would match what is observed (see Liebert et al. 1994; Landsman et al. 1998; Brown 2004). So to the extent that the model here explains the anomalies in that system, it can also account for the UVX. In contrast, it has been shown that the UVX cannot be reproduced by the sum of GC populations (van Albada et al. 1981; Bica & Alloin 1988; Davidsen & Ferguson 1992; Dorman et al. 1995). Most other alternative explanations have been ruled out, including: metal-poor populations (references above and Rose 1985), white dwarfs (Landsman et al. 1998), and “blue stragglers” (Bailyn & Pinsonneault 1995).

It is also well-established that the UVX is stronger in more metal-rich galaxies (Faber 1983; Burstein et al. 1988); this is a natural prediction of the mechanism here, since the enhanced abundances imply higher mean dust-to-gas ratios, making the process

we describe easier (more widespread) and more strongly observable (since the absolute metallicities of the “enhanced” stars are much larger). More recently, it has been observed that there is a good correlation between the UVX and C and Na abundances, while there is not a strong correlation with Fe (Rich et al. 2005); in particular in the UVX systems it seems that the light-element abundances fluctuate *independent* from the heavier elements (McWilliam 1997; Worthey 1998; Greggio & Renzini 1999; Donas et al. 2007), exactly as predicted here. Additional properties such as the lack of strong environmental dependence, weak redshift evolution, and large dispersion in UVX populations, are consistent with our scenario (Brown 2004; Atlee et al. 2009).

### 4.5 Dust-to-Gas Variations in GMCs and Nearby Galaxies

The model here predicts large variations in the dust-to-gas ratio in the star-forming molecular gas, under the right conditions. But as noted in (3), these fluctuations will not manifest in the most obvious manner (via extinction mapping). However, there are some tracers sensitive to large grains, for example in the sub-millimeter. One tentative example which might show this behavior is the extreme nuclear region of NGC 1266. Several authors (see e.g. Alatalo et al. 2011; Pellegrini et al. 2013; Nyland et al. 2013) have pointed out a number of unusual properties in this galaxy, one of which is that the molecular gas in the nucleus, and dust traced specifically by the sub-millimeter imaging, are not necessarily co-spatial (in some sub-regions they are, in others there are significant offsets). It is worth noting that the nuclear region of this system is probably well in the regime we describe here, with properties ( $T_{10} \sim 10$ ,  $\Sigma_{300} \sim 40$ ,  $Q \sim 2$ ,  $R_{10} \sim 10$ ; see references above) that imply large fluctuations within any clouds or sub-clouds with sizes above a few parsec (masses  $\gtrsim 10^6 M_\odot$ ).

### 4.6 Consequences for Planet Formation

If this mechanism operates, it can have dramatic implications for planet formation in the proto-stellar/proto-planetary disks which form from the affected cores. Many models of terrestrial planet formation, for example, predict far more efficient planet formation at enhanced metallicities (via either simplistic grain growth/accretion, or the onset of instabilities such as the streaming instability; see references in § 1). For example, in the simulations of (Bai & Stone 2010c), and analytic models in e.g. (Cuzzi et al. 2010; Hopkins 2014), there is an exponential increase in the maximum density of solids reached (enough to allow some to become self-gravitating planetesimals) if the initial disk metallicity is a few times solar – this is sufficient such that, once the metals grow in the disk into more massive grains and sediment into the midplane, their density becomes larger than that of the midplane gas, triggering a range of new dust-clumping instabilities. Such metallicity enhancements are relatively modest, compared to the extremes we have discussed above. And in the most extreme cases we predict ( $Z \sim 100 Z_\odot$ ), these instabilities would operate not just in the midplane but everywhere in the disk, almost instantaneously upon its formation!

Even if the mechanisms of planet formation remain uncertain, there is an increasingly well-established correlation between giant planet occurrence rates and stellar metallicity (see e.g. Johnson et al. 2010, and references therein). Whatever causes this, it is clear that stellar abundance variations – seeded before both the star and protoplanetary disk form – must be accounted for in understanding the occurrence rates and formation conditions of giant planets. One might predict, for example, a dramatic increase in the occurrence rates of planets in the sorts of open clusters which formed in very massive, large clouds, similar to NGC 6791 discussed above;



in these circumstances the occurrence rate might have more to do with the statistics of seeded dust abundance variations, than with the planet formation mechanisms themselves.

Particularly interesting, our model does not just predict a uniform variation in metallicities (as is usually assumed when modeling planet formation under “high” or “low” metallicity conditions). Rather, we specifically predict abundance variations in the species preferentially concentrated in the largest grains in large, cold clouds. So we predict there should be disks preferentially concentrated in carbonaceous grains, for example. Similarly, if ice mantles form, there will be disks with over-abundances of oxygen. And if the progenitor cloud was slightly larger still, silicates can be preferentially enhanced (relative to species like iron). So it is actually possible, under the right conditions, to form a proto-planetary disk which is highly enhanced in large carbonaceous and silicate grains, even while the host star exhibits apparently “normal” abundances of iron and most other species. This will radically change the chemistry of the massive grains which form in the disk, hence the conditions (and mechanisms) of planet formation, as well as the composition of the resulting planets!

## 5 FUTURE WORK

Our intent here is to highlight a new and (thus far) unexplored physical process by which unusual abundance patterns may be seeded in stars formed in massive molecular clouds. Many consequences of this should be explored in more detail.

Predicting more accurately the abundance patterns imprinted by this process requires combining the calculations above (for grain density fluctuations as a function of grain size) with detailed, explicit models for the grain chemistry. Specifically, knowing the abundance of different elements, integrated over all large grains above some minimum  $a_{\mu}$ , would enable strong quantitative predictions for relative fluctuation amplitudes of different abundances. At the moment this is extremely uncertain and model-dependent, since the chemical structures of large grains in particular are difficult to probe and often degenerate (for a discussion, see Draine 2003; Zubko et al. 2004).

Another critical next step is to directly simulate the formation of proto-stellar cores in a GMC while explicitly following a size distribution of grains as aerodynamic particles. This would remove many current uncertainties in the non-linear grain clustering amplitudes: the analytic model here is a reasonable approximation to existing simulations but cannot capture the full range of behaviors and subtle correlations between the velocity and density fields in turbulence, as well as the more complicated mutual role of gas density fluctuations seeding core formation while independent grain density fluctuations occur alongside. Probably the most poorly-understood element of the physics here is how the instabilities we describe are modified in the presence of a magnetic field (§ 2.3). If most of the grains are weakly charged (which is by no means certain); we would then expect them to go through alternating phases of neutral and charged as they collide with electrons and ions, “seeing” a non-linearly fluctuating magnetic force. Properly modeling this requires (in addition to the physics above) magnetohydrodynamic turbulence with non-ideal MHD (given the ionization fractions in regions of interest), explicit treatment of grain-electron interactions/capture, and subsequent capture-dependent grain-MHD interactions.

But any such simulations remain very challenging. Almost all current molecular cloud simulations treat grains (if at all) by assuming either a constant dust-to-metals ratio, or as a fluid (the two-

fluid approximation; see e.g. Downes 2012). In these approximations, the physical processes driving dust-to-gas ratio fluctuations (the subject of this paper) are artificially prohibited. It has only just become possible to follow grains as aerodynamic species in astrophysical codes (the most basic requirement to see the behavior here), and while this has been applied to idealized fluid dynamics and proto-planetary disk simulations (§ 1) this has not yet been extended to GMC scales. No such simulations have included all the MHD effects described above. The resolution also remains challenging; simulations must be able to resolve sub/trans-sonic turbulent eddies with scales down to about  $\sim 0.05$  times the critical scale ( $R_{\text{crit}}$ ) for convergence (Hopkins 2013b), which here is the scale of individual cores, while still capturing the cloud-scale dynamics such that a statistical population of cores can be tracked.

It is also important to explore the predictions for stellar properties. Stellar evolution models have not, in general, considered the case of stars forming from regions super-enhanced in certain species, let alone stars with an order-unity *initial* mass fraction in heavy elements. Knowing whether these would simply appear as stars which have completed light-element burning, or would produce unique observational signatures, would enable powerful tests of the scenario outlined here as well as providing a new window into extreme stellar physics.

## ACKNOWLEDGMENTS

We thank Jessie Christiansen, Selma de Mink, and Charlie Conroy for many helpful discussions and sanity checks during the development of this work. Partial support for PFH was provided by the Gordon and Betty Moore Foundation through Grant #776 to the Caltech Moore Center for Theoretical Cosmology and Physics.

## REFERENCES

- Abia, C., Domínguez, I., Gallino, R., Busso, M., Masera, S., Straniero, O., de Laverny, P., Plez, B., & Isern, J. 2002, *ApJ*, 579, 817
- Abia, C., & Isern, J. 2000, *ApJ*, 536, 438
- Alatalo, K., et al. 2011, *ApJ*, 735, 88
- Atlee, D. W., Assef, R. J., & Kochanek, C. S. 2009, *ApJ*, 694, 1539
- Bai, X.-N., & Stone, J. M. 2010a, *ApJ*, 722, 1437
- . 2010b, *ApJS*, 190, 297
- . 2010c, *ApJL*, 722, L220
- Bailyn, C. D., & Pinsonneault, M. H. 1995, *ApJ*, 439, 705
- Barkana, R., & Loeb, A. 2001, *Physics Reports*, 349, 125, review reionization
- Bastian, N., Cabrera-Ziri, I., Davies, B., & Larsen, S. S. 2013a, *MNRAS*, in press, arXiv:1309.5092
- Bastian, N., Lamers, H. J. G. L. M., de Mink, S. E., Longmore, S. N., Goodwin, S. P., & Gieles, M. 2013b, *MNRAS*, in press, arXiv:1309.3566
- Bate, M. R., & Bonnell, I. A. 2005, *MNRAS*, 356, 1201
- Bec, J., Biferale, L., Cencini, M., Lanotte, A. S., & Toschi, F. 2009, eprint arxiv:0905.1192
- Bec, J., Cencini, M., Hillerbrand, R., & Turitsyn, K. 2008, *Physica D Nonlinear Phenomena*, 237, 2037
- Bergeat, J., Knapik, A., & Rutily, B. 2002a, *A&A*, 390, 967
- . 2002b, *A&A*, 385, 94
- Bica, E., & Alloin, D. 1988, *A&A*, 192, 98
- Blanco, V. M. 1965, in *Galactic Structure*; Edited by Adriaan Blaauw and Maarten Schmidt. Published by the University of Chicago Press, Chicago, IL, ed. A. Blaauw & M. Schmidt, 241

- Bolatto, A. D., Leroy, A. K., Rosolowsky, E., Walter, F., & Blitz, L. 2008, *ApJ*, 686, 948
- Bracco, A., Chavanis, P. H., Provenzale, A., & Spiegel, E. A. 1999, *Physics of Fluids*, 11, 2280
- Bragaglia, A., Gratton, R. G., Carretta, E., D’Orazi, V., Sneden, C., & Lucatello, S. 2012, *A&A*, 548, A122
- Brown, T. M. 2004, *Astrophysics and Space Science*, 291, 215
- Burgers, J. 1973, *The nonlinear diffusion equation: asymptotic solutions and statistical problems* (D. Reidel Pub. Co.)
- Burstein, D., Bertola, F., Buson, L. M., Faber, S. M., & Lauer, T. R. 1988, *ApJ*, 328, 440
- Carballido, A., Stone, J. M., & Turner, N. J. 2008, *MNRAS*, 386, 145
- Carraro, G. 2013, *ArXiv e-prints*, arXiv:1308.5195
- Carrera, R. 2012, *ApJ*, 758, 110
- Carrera, R., & Martinez-Vazquez, C. E. 2013, *A&A*, in press, arXiv:1308.4548
- Carretta, E., Bragaglia, A., Gratton, R., & Lucatello, S. 2009a, *A&A*, 505, 139
- Carretta, E., et al. 2009b, *A&A*, 505, 117
- . 2013, *A&A*, 557, A138
- Conroy, C., & Spergel, D. N. 2011, *ApJ*, 726, 36
- Cuzzi, J. N., Hogan, R. C., & Bottke, W. F. 2010, *Icarus*, 208, 518
- Cuzzi, J. N., Hogan, R. C., Paque, J. M., & Dobrovolskis, A. R. 2001, *ApJ*, 546, 496
- Davidsen, A. F., & Ferguson, H. C. 1992, in *Physics of Nearby Galaxies: Nature or Nurture?*; Proceedings of the 27th Rencontre de Moriond, Les Arcs, France, March 15-22, 1992. Edited by Trinh Xuan Thuan, Chantal Balkowski, and J. Tran Thanh Van. Gif-sur-Yvette: Editions Frontieres, ed. T. X. Thuan, C. Balkowski, & J. Tran Thanh Van, 125
- D’Ercole, A., Vesperini, E., D’Antona, F., McMillan, S. L. W., & Recchi, S. 2008, *MNRAS*, 391, 825
- Dittrich, K., Klahr, H., & Johansen, A. 2013, *ApJ*, 763, 117
- Dominy, J. F. 1984, *ApJS*, 55, 27
- Donas, J., et al. 2007, *ApJS*, 173, 597
- Dorman, B., O’Connell, R. W., & Rood, R. T. 1995, *ApJ*, 442, 105
- Downes, T. P. 2012, *MNRAS*, 425, 2277
- Draine, B. T. 2003, *ARA&A*, 41, 241
- Draine, B. T., & Li, A. 2007, *ApJ*, 657, 810
- Draine, B. T., & Sutin, B. 1987, *ApJ*, 320, 803
- Elmegreen, B. G. 1979, *ApJ*, 232, 729
- Faber, S. M. 1983, *Highlights of Astronomy*, 6, 165
- Federrath, C., Klessen, R. S., & Schmidt, W. 2008, *ApJL*, 688, L79
- Fessler, J. R., Kulick, J. D., & Eaton, J. K. 1994, *Physics of Fluids*, 6, 3742
- Frinchaboy, P. M., Marino, A. F., Villanova, S., Carraro, G., Majewski, S. R., & Geisler, D. 2008, *MNRAS*, 391, 39
- Geisler, D., Villanova, S., Carraro, G., Pilachowski, C., Cummings, J., Johnson, C. I., & Bresolin, F. 2012, *ApJL*, 756, L40
- Greggio, L., & Renzini, A. 1999, *Memorie della Societa Astronomica Italiana*, 70, 691
- Gualtieri, P., Picano, F., & Casciola, C. M. 2009, *Journal of Fluid Mechanics*, 629, 25
- Guelin, M., Langer, W. D., Snell, R. L., & Wootten, H. A. 1977, *ApJL*, 217, L165
- Gustavsson, K., Meneguz, E., Reeks, M., & Mehlig, B. 2012, *New Journal of Physics*, 14, 115017
- Hennebelle, P., & Chabrier, G. 2008, *ApJ*, 684, 395
- Heyer, M., Krawczyk, C., Duval, J., & Jackson, J. M. 2009, *ApJ*, 699, 1092
- Hogan, R. C., & Cuzzi, J. N. 2007, *Phys. Rev. E*, 75, 056305
- Hogan, R. C., Cuzzi, J. N., & Dobrovolskis, A. R. 1999, *Phys. Rev. E*, 60, 1674
- Hopkins, P. F. 2012a, *MNRAS*, in press, arXiv:1211.3119
- . 2012b, *MNRAS*, 423, 2037
- . 2012c, *MNRAS*, in press [arXiv:1204.2835]
- . 2013a, *MNRAS*, 430, 1653
- . 2013b, *MNRAS*, in press, arXiv:1307.7147
- . 2013c, *MNRAS*, 428, 1950
- . 2014, *MNRAS*, in press, arXiv:1401.2458
- Hoppe, P., & Zinner, E. 2000, *Journal of Geophysical Research*, 105, 10371
- Horch, E., Demarque, P., & Pinsonneault, M. 1992, *ApJL*, 388, L53
- Hynes, K. M., & Gyngard, F. 2009, in *Lunar and Planetary Inst. Technical Report*, Vol. 40, Lunar and Planetary Institute Science Conference Abstracts, 1198
- Izzard, R. G., Jeffery, C. S., & Lattanzio, J. 2007, *A&A*, 470, 661
- Jalali, M. A. 2013, *ApJ*, in press, arXiv:1301.2064
- Johansen, A., & Youdin, A. 2007, *ApJ*, 662, 627
- Johansen, A., Youdin, A. N., & Lithwick, Y. 2012, *A&A*, 537, A125
- Johnson, J. A., Aller, K. M., Howard, A. W., & Crepp, J. R. 2010, *PASP*, 122, 905
- Klessen, R. S., & Burkert, A. 2000, *ApJS*, 128, 287
- . 2001, *ApJ*, 549, 386
- Knapp, G., Pourbaix, D., & Jorissen, A. 2001, *A&A*, 371, 222
- Konstantin, L., Girichidis, P., Federrath, C., & Klessen, R. S. 2012, *ApJ*, 761, 149
- Krumholz, M. R., & McKee, C. F. 2005, *ApJ*, 630, 250
- Landsman, W., Bohlin, R. C., Neff, S. G., O’Connell, R. W., Roberts, M. S., Smith, A. M., & Stecher, T. P. 1998, *AJ*, 116, 789
- Langer, W. D., Wilson, R. W., Henry, P. S., & Guelin, M. 1978, *ApJL*, 225, L139
- Larsen, S. S., Strader, J., & Brodie, J. P. 2012, *A&A*, 544, L14
- Li, A., & Draine, B. T. 2001, *ApJ*, 554, 778
- Liebert, J., Saffer, R. A., & Green, E. M. 1994, *AJ*, 107, 1408
- Lyra, W., & Kuchner, M. 2013, *Nature*, 499, 184
- Martell, S. L., & Smith, G. H. 2009, *PASP*, 121, 577
- Mathis, J. S., Ruml, W., & Nordsieck, K. H. 1977, *ApJ*, 217, 425
- McClure, R. D. 1997, *PASP*, 109, 256
- McWilliam, A. 1997, *ARA&A*, 35, 503
- Mocák, M., Müller, E., Weiss, A., & Kifonidis, K. 2009, *A&A*, 501, 659
- Monaco, L., Villanova, S., Bonifacio, P., Caffau, E., Geisler, D., Marconi, G., Momany, Y., & Ludwig, H.-G. 2012, *A&A*, 539, A157
- Monchaux, R., Bourgoïn, M., & Cartellier, A. 2010, *Physics of Fluids*, 22, 103304
- Monchaux, R., Bourgoïn, M., & Cartellier, A. 2012, *International Journal of Multiphase Flow*, 40, 1
- Muno, M. P., Law, C., Clark, J. S., Dougherty, S. M., de Grijs, R., Portegies Zwart, S., & Yusef-Zadeh, F. 2006, *ApJ*, 650, 203
- Nyland, K., et al. 2013, *ApJ*, 779, 173
- Olla, P. 2010, *Phys. Rev. E*, 81, 016305
- Padoan, P., & Nordlund, Å. 2011, *ApJ*, 730, 40
- Pan, L., Padoan, P., Scalo, J., Kritsuk, A. G., & Norman, M. L. 2011, *ApJ*, 740, 6
- Pancino, E., Carrera, R., Rossetti, E., & Gallart, C. 2010, *A&A*, 511, A56

- Pellegrini, E. W., et al. 2013, *ApJL*, 779, L19
- Piersanti, L., Cabezón, R. M., Zamora, O., Domínguez, I., García-Senz, D., Abia, C., & Straniero, O. 2010, *A&A*, 522, A80
- Piotto, G., et al. 2007, *ApJL*, 661, L53
- Rich, R. M., et al. 2005, *ApJL*, 619, L107
- Rose, J. A. 1985, *AJ*, 90, 1927
- Rouson, D. W. I., & Eaton, J. K. 2001, *Journal of Fluid Mechanics*, 428, 149
- Sana, H., Momany, Y., Gieles, M., Carraro, G., Beletsky, Y., Ivanov, V. D., de Silva, G., & James, G. 2010, *A&A*, 515, A26
- Seale, J. P., Looney, L. W., Wong, T., Ott, J., Klein, U., & Pineda, J. L. 2012, *ApJ*, 751, 42
- Shane, C. D. 1928, *Lick Observatory Bulletin*; Berkeley : University of California Press, 13, 123
- Squires, K. D., & Eaton, J. K. 1991, *Physics of Fluids A: Fluid Dynamics*, 3, 1169
- Stephenson, C. B. 1973, *A general catalogue of S stars* (Cleveland Publications of the Warner and Swasey Observatory, Cleveland, Ohio: Case Western Reserve University)
- Twarog, B. A., Carraro, G., & Anthony-Twarog, B. J. 2011, *ApJL*, 727, L7
- van Albada, T. S., de Boer, K. S., & Dickens, R. J. 1981, *MNRAS*, 195, 591
- Watson, W. D., Snyder, L. E., & Hollis, J. M. 1978, *ApJL*, 222, L145
- Weingartner, J. C., & Draine, B. T. 2001, *ApJ*, 548, 296
- Wilkinson, M., Mehlig, B., & Gustavsson, K. 2010, *EPL (Europhysics Letters)*, 89, 50002
- Wolfire, M. G., Hollenbach, D., McKee, C. F., Tielens, A. G. G. M., & Bakes, E. L. O. 1995, *ApJ*, 443, 152
- Worthey, G. 1998, *PASP*, 110, 888
- Yoshimoto, H., & Goto, S. 2007, *Journal of Fluid Mechanics*, 577, 275
- Youdin, A. N., & Goodman, J. 2005, *ApJ*, 620, 459
- Zaichik, L. I., & Alipchenkov, V. M. 2009, *New Journal of Physics*, 11, 103018
- Zamora, O., Abia, C., Plez, B., Domínguez, I., & Cristallo, S. 2009, *A&A*, 508, 909
- Zhang, X., & Jeffery, C. S. 2013, *MNRAS*, 430, 2113
- Zinner, E. 2014, *Treatise on Geochemistry* (Book - Elsevier Ltd., Oxford; eds. H. D. Holland and K. K. Turekian), 1.4, 181
- Zubko, V., Dwek, E., & Arendt, R. G. 2004, *ApJS*, 152, 211